Spin Densities and Polymerizabilities of Aniline Derivatives Deduced from Density Functional Calculations

G. D'Aprano,[†,‡] E. Proynov,[‡] M. Lebœuf,[‡,§] M. Leclerc,[‡] and D. R. Salahub*[,‡,§]

Contribution from the Département de chimie, Université de Montréal, C.P. 6128, Succ. Centre-ville, Montréal, Québec H3C 3J7, Canada, and CERCA (Centre de Recherche en Calcul Appliqué), 5160 boul. Décarie, bureau 400, Montréal, Québec H3X 2H9, Canada

Received November 14, 1995. Revised Manuscript Received May 24, 1996[⊗]

Abstract: A theoretical study of the electronic structure of some aniline derivatives is performed, aimed at a microscopic explanation of the observed polymerizability of these compounds. Monomers with methyl and methoxy substituents located at various positions on the benzenoid ring are considered using the density functional theory program deMon-KS. The calculations indicate that the distribution of the net radical cation spin among the atoms (atomic spin populations) is very sensitive to the nature and the position of the substituents. In fact this distribution reflects specifics of the electronic structure of these monomers related to their polymerizability. It is shown that polymerization is favored when the net spin population on the nitrogen atom is similar to that on the ring carbon atom at the *para* position. On the contrary, in the species that do not polymerize, these two atoms have substantially different spin populations. A possible explanation of this result is discussed in terms of chemical reactivity based on the softness−hardness concept.

Introduction

It has been known for more than a century that aniline undergoes oxidative polymerization in acidic aqueous solution.[1] More recently, Diaz *et al*. have reported that electrooxidation of aniline also gives rise to an electroactive polyaniline.[2] In all cases, the oxidatively activated polymerization is an efficient means of head-to-tail bond formation, viz. a chemical bond between the nitrogen atom and the ring carbon atom at the *para* position.[3]

Many publications have indicated that polyaniline exhibits an increase of its electrical conductivity by ten orders of magnitude, either by a simple protonation,[4] or by oxidative chemical or electrochemical doping.[5] Furthermore, this material exhibits electrochromic effects, changing from pale yellow to green, to blue-violet.[2,4,5] The reversibility of these unusual electrical and optical properties and the low cost of fabrication make this polymer very attractive for implementation in various technological devices, such as biosensors,[6] light-emitting diodes,[7] molecular devices,[8] conducting photoresists,[9] optical switches,[10] smart windows,[11] and others. These emerging potential applications have motivated efforts to improve the processability and environmental stability. Structural modification has mainly been exploited to achieve such goals. For example, alkyl or alkoxy side groups have been introduced either in the benzenoid ring or on the nitrogen atom.[12]

In the course of previous studies, several aniline derivatives were investigated,[13−15] varying the nature (alkyl vs alkoxy) and the position (2- vs 3,5-position) of the substituents. These studies have shown that alkoxy groups at the 3- or 5-position (*meta* ring carbon atoms) do not yield electroactive polymers,[14] which is also in agreement with previous results reported by Lacroix *et al*.[16] One might suppose that the presence of an alkoxy group at the *meta* positions drives the electron (spin) density distribution among the ring carbon atoms and the nitrogen atom in a manner that is unfavorable for polymerization. However, it is not obvious whether the influence of such groups on the polymerizability is predominantly at the electronic level or simply due to steric effects. To gain more detailed insight into this matter, reliable quantum chemical calculations of the electronic structure of these compounds are necessary.

In the present work, we use an *ab initio* quantum chemical method based on density functional theory (DFT) (the program deMon-KS[23,25]) to investigate the electronic effects of various substituents on the distribution of the unpaired-electron spin-density about potentially reactive sites of the considered radical cations (Figure 1), namely, 2-methoxyaniline (2MOA), 3-methoxyaniline (3MOA), 2-methoxy-5-methylaniline (MOMA),

* To whom correspondence should be addressed.
† Present address: Max-Planck-Institut für Polymerforschung, Ackermannweg 10, D 55021 Mainz, Postfach 3148, Germany.
‡ Université de Montréal.
§ CERCA.
⊗ Abstract published in *Advance ACS Abstracts,* September 15, 1996.

(1) Letheby, H. *J. Chem. Soc.* **1862**, *15*, 161.
(2) Diaz, A. F.; Logan, A. J. *J. Electroanal. Chem.* **1980**, *111*, 111.
(3) Waltman, R. J.; Bargon, J. *Can. J. Chem.* **1986**, *64*, 76.
(4) (a) De Surville, R.; Jozefowicz, M.; Yu, L. T.; Périchon, J.; Buvet, J. *Electrochim. Acta* **1968**, *13*, 145. (b) Chiang, J. C.; MacDiarmid, A. G. *Synth. Met.* **1986**, *13*, 193.
(5) *Handbook of Conducting Polymers*; Skotheim, T. A., Ed.; Marcel Dekker: New York, 1986.
(6) (a) Hoa, D. T.; Kumar, T. N. S.; Punekar, N. S.; Srinivasa, R. S.; Lal, R.; Contractor, A. Q. *Anal. Chem.* **1992**, *64*, 2645. (b) Deshpande, M. V.; Amalnerkar, D. P. *Prog. Polym. Sci.* **1993**, *18*, 623.
(7) Gustafsson, G.; Cao, Y.; Treacy, G. M.; Klavetter, F.; Colaneri, N.; Heeger, A. J. *Nature* **1992**, *357*, 477.
(8) Lotan, N.; Ashkenazi, G.; Tuchman, S.; Nehamkin, S.; Sideman, S. *Mol. Cryst. Liq. Cryst.* **1993**, *236*, 95.
(9) (a) Venugopal, G.; Quan, X.; Johnson, G. E.; Houlihan, F. M.; Chin, E.; Nalamasu, O. *Chem. Mater.* **1995**, *7*, 271. (b) Angelopoulos, M.; Shaw, J. M.; Huang, W. S.; Kaplan, R. D. *Mol. Cryst. Liq. Cryst.* **1990**, *189*, 221.
(10) (a) Osaheni, J. A.; Jenekhe, S. A.; Vanherzeele, H.; Meth, J. S.; Sun, Y.; MacDiarmid, A. G. *J. Phys. Chem.* **1992**, *96*, 2830. (b) Callender, C. L.; Robitaille, L.; Leclerc, M. *Opt. Eng. (Bellingham, Wash.)* **1993**, *32*, 2246.
(11) Hyodo, K. *Electrochim. Acta* **1994**, *39*, 265.
(12) Diaz, A. F.; Nguyen, M. T.; Leclerc, M. In *Electronically Conducting Soluble Polymers*; Marcel Dekker: New York, 1995; p 555.
(13) D'Aprano, G.; Leclerc, M.; Zotti, G.; Schiavon, G. *Chem. Mater.* **1995**, *7*, 33.
(14) D'Aprano, G.; Leclerc, M.; Zotti, G. *J. Electroanal. Chem.* **1993**, *351*, 145. D'Aprano, G. Ph.D. Thesis, Université de Montréal, 1994.
(15) D'Aprano, G.; Leclerc, M.; Zotti, G. *Macromolecules* **1992**, *25*, 2145.
(16) Lacroix, J. C.; Garcia, P.; Audière, J. P.; Clément, R.; Kahn, O. *Synth. Met.* **1991**, *44*, 117.

S0002-7863(95)03819-4 CCC: $12.00

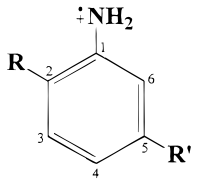

R = R' = H (ANI)
R = OCH_3, R' = H (2MOA)
R = H, R' = OCH_3 (3MOA)
R = OCH_3, R' = CH_3 (MOMA)
R = CH_3, R' = OCH_3 (MMOA)
R = R' = OCH_3 (DMOA)
R = R' = CH_3 (DMA)

Figure 1. The different monomers studied.

2-methyl-5-methoxyaniline (MMOA), 2,5-dimethoxyaniline (DMOA), and 2,5-dimethylaniline (DMA). The theoretical background and the details of the calculations are described in the next section.

Computational Method

Only a few quantum chemical studies of aniline derivatives in relation to their polymerizability are available.[17−19] Because of the relatively large size of these molecules, correlation-based ab-initio methods have not been employed. Furthermore, the electronic structure of radical cations is known to be difficult even for the most sophisticated *ab initio* methods. Electron correlation has proven to play a crucial role in determining the spatial distribution and localization of the electron and spin densities, and the equilibrium geometry of hydrocarbon radicals, especially radical cations.[21,22] This fact reflects the need to include electron correlation at a high level, in order to calculate accurately the hyperfine structures of such radical systems.[21,22] Conjugated radicals usually possess a broken (spatial- and/or spin-) symmetry with respect to the parent neutral molecule.[20]

Among the first principles methods including electron correlation, density functional theory has become increasingly popular, mainly due to its progressively improved accuracy at less computational cost than other correlated *ab initio* methods.[23,24] In the present study we investigate the electronic structure of the considered aniline derivatives using the *linear combination of Gaussian-type orbital Kohn−Sham DFT* (LCGTO-KS-DFT) program deMon-KS[23,25] The program handles the DFT variational problem by solving the Kohn-Sham system of equations. These DFT equations resemble in structure and numerical realization the Hartree−Fock (HF) equations widely used in quantum chemistry. However, while the Hartree−Fock equations do not involve electron correlation, and by construction give only approximate results for the electronic structure, the Kohn−Sham DFT equations are in principle exact for the ground state, and electron correlation is taken explicitly into account via the exchange-correlation functional. If the exact form of this functional were known, the KS-DFT method would yield the exact energy and other ground state properties of a molecule. In practice, approximate exchange-correlation functionals are devised and used, and their accuracy determines the quality of the DFT results. In this study we use mainly the local spin density approximation (LSD) for the exchange-correlation term. This widely used approximation in Kohn−Sham DFT is based on the assumption that the electron correlation in a molecule resembles locally (at any given point) the correlation in a homogeneous electron gas having a density equal to the molecular electron density at that point (see refs 23 and 24 for more theoretical details). This approximation has been successfully applied in molecular and solid-state DFT calculations. One should keep in mind that the LSD tends to overestimate the binding energy of molecules, and for the needs of thermochemistry one has to employ more sophisticated (and computationally more expensive) nonlocal functionals,[24,26,27] involving not only the electron density but also its spatial gradients within the so-called Generalized Gradient Approximation (GGA). We present below results from such nonlocal GGA calculations as well, for the key example of aniline. More important for the present study is the fact that the LSD approximation often yields reasonably good equilibrium geometries and electron spin density distributions.[20−22] Concerning organic radicals, the LSD has been successfully applied to calculate the electronic structure and the geometry of the allyl radical and the odd (neutral) polyene radicals C_5H_7 to $C_{11}H_{13}$ within the LCGTO-KS-DFT code deMon-KS.[20] The LSD results correctly predicted the alternation of the single and double C−C bonds along the polymer chain. The electron spin-density distribution was also in line with experimental data showing the formation of a "soliton-like" structure.[20] Recently, the program deMon-KS has been successfully employed to study the hyperfine coupling structures of a set of hydrocarbon radicals and radical cations.[21,22] It was shown that the LSD approximation gives on average very good results for the hyperfine structures and equilibrium geometries of such radicals, although GGA corrections were necessary in some cases to further improve the isotropic hyperfine coupling constants on carbon atoms.[21,22]

In the present work we give some evidence that the real space distribution of the unpaired-electron spin-density is a crucial property determining the polymerizability of the considered aniline derivatives. After this work was completed, we became aware of the very recent study of Smith *et al.*[19] in which the LSD approximation (using the program DMol[28]) was successfully applied to investigate the polymerizability trends of pyrrole, thiophene, and (*E*)-stilbene based radical cations. It was shown that the calculated unpaired-electron spin-density distribution in such cations contains important information and can be used to predict reaction sites in the polymerization process. Below we show that, for the case of the aniline derivatives, just calculating the values of the unpaired spin-density is not enough to explain the subtleties associated with the polymerizabilities of these compounds. Additional theoretical concepts, such as softness−hardness and the Fukui function concepts in DFT, provide important insight.

All the calculations discussed in the present work were carried out with the LCGTO-KS-DFT code deMon-KS[23,25] on Silicon Graphics R4000 workstations. Orbital basis sets of DZVP quality were used with added polarization functions:[29] (621/41/1*) for C, O, and N atoms, and (41/1*) for H atoms. The auxiliary basis sets used to fit analytically the electron density and the exchange-correlation potential (for the sake of simplifying the calculation of the multicenter integrals) were as follows: (5,2;5,2) for C and N; (4,4;4,4) for O; and (5,1;5,1) for H atoms (standard basis set notations are used, as described in refs 25 and 29).

Results and Discussion

For the sake of validation of the computational method used, we have first calculated the electronic and geometric structure of aniline (the parent monomer), for which experimental data

(17) Davis, T. P.; Rogers, S. C. *Eur. Polym. J.* **1993**, *29*, 1311.
(18) Lacroix, J. C.; Garcia, P.; Audiere, J. P.; Clement, R.; Kahn, O. *New J. Chem.* **1990**, *14*, 87.
(19) Smith, J. R.; Cox, P. A.; Campbell, S. A.; Ratcliffe, N. M. *J. Chem. Soc., Faraday Trans.* **1995**, *91*, 2331.
(20) Sim, F.; Salahub, D. R.; Chin, S.; Dupuis, M. *J. Chem. Phys.* **1991**, *95*, 4317.
(21) Eriksson, L. A.; Malkin, V. G.; Malkina, O. L.; Salahub, D. R. *J. Chem. Phys.* **1993**, *99*, 9756.
(22) Eriksson, L. A.; Malkin, V. G.; Malkina, O. L.; Salahub, D. R. *Int. J. Quantum Chem.* **1994**, *52*, 879.
(23) Salahub, D. R.; Castro, M. E.; Proynov, E. I. In *Relativistic and Electron Correlation Effects in Molecules and Solids*; NATO ASI Series B: Physics, Vol. 318; Malli, G. L., Ed.; Plenum Press: New York, 1994.
(24) Parr, R. G.; Yang, W. *Density−Functional Theory of Atoms and Molecules*; Oxford University Press: New York; Clarendon Press: Oxford, 1989.
(25) St-Amant, A.; Salahub, D. R. *Chem. Phys. Lett.* **1990**, *169*, 387. St-Amant, A. Ph.D. Thesis Université de Montréal, 1992.
(26) Perdew, J. P.; Wang, Y. *Phys. Rev. B* **1986**, *33*, 8800.
(27) Perdew, J. P. *Phys. Rev. B* **1986**, *33*, 8822; *34*, 7406.
(28) DMol; A Density Functional Theory Program within the Insight II Molecular Modelling Package; Biosym Technologies Inc.: San Diego, 1993.
(29) Godbout, N.; Salahub, D. R.; Andzelm, J.; Wimmer, E. *Can. J. Chem.* **1992**, *70*, 560.

Table 1. Bond Distances (R [Å]) and Bond Orders (P) of Aniline and Aniline Radical Cation Obtained within the LSD and GGA Approximations

aniline	method	R_{N-C_1}	$R_{C_1-C_2}$	$R_{C_2-C_3}$	$R_{C_3-C_4}$	P_{N-C_1}	$P_{C_1-C_2}$	$P_{C_2-C_3}$	$P_{C_3-C_4}$
neutral	LSD	1.371	1.406	1.391	1.397	1.13	1.35	1.51	1.46
	GGA	1.392	1.419	1.404	1.409	1.14	1.37	1.52	1.46
	EXP[a]	1.402	1.397	1.394	1.396				
cation	LSD	1.335	1.430	1.374	1.412	1.32	1.18	1.58	1.32
	GGA	1.351	1.445	1.386	1.426	1.34	1.19	1.59	1.32

[a] Data from ref 30.

have been reported.[30] Table 1 contains the calculated bond distances of aniline versus the experimental values. The calculated electronic structure of the different aniline derivatives is then compared to the structure of the parent monomer.

The calculations for aniline were done both at the LSD level (with the Vosko, Wilk, and Nusair (VWN) version for the correlation energy[31]) and by using a more sophisticated GGA exchange-correlation scheme: the GGA exchange functional of Perdew and Wang,[26] combined with the GGA correlation functional of Perdew.[27] As seen from Table 1, the bond distances obtained within the LSD approximation are in general very close to the experimental values, and also to the GGA results. An exception is the N−C bond distance where the LSD yields a somewhat shorter value, compared to experiment and the GGA. The bond orders for all N−C and C−C bonds evaluated at the LSD level are very close to the corresponding GGA results. Both the LSD and the GGA approximations predict the same trend in changing the benzenoid ring geometry upon formation of the radical cation. In neutral aniline, the C−C bond lengths are almost equal, in agreement with the experimental data (Table 1), and the symmetry of the benzenoid ring is well preserved. In the radical cation, the benzenoid ring symmetry is broken: the C_2-C_3 and C_5-C_6 bonds are noticeably shorter than the others, while the C_1-C_2 and C_6-C_1 bonds are longer than the others. This situation is reflected also in the inequality of the C−C bond orders in the aniline radical cation (Table 1).

The effective atomic charges of the aniline radical cation within the LSD approximation (Table 2) are close to the corresponding GGA values. In our spin-polarized calculations, the effective atomic charges are estimated via the standard Mulliken population analysis, as implemented in deMon-KS.[25] A quantity of prime importance, as discussed below, is the distribuition of the radical cation unpaired spin-density among the atoms. This distribution is estimated in two different ways: First we look at the real space distribution of the spin density:

$$n_s(\mathbf{r}) = n_\uparrow(\mathbf{r}) - n_\downarrow(\mathbf{r}) \quad (1)$$

where $n_\uparrow$, $n_\downarrow$ denote the electron density for the corresponding spin direction. The distribution of n_s is calculated numerically on a set of grid points in real space. Figures 2 and 3 show the three-dimensional real-space distribution of $n_s(\mathbf{r})$ in some of the aniline derivatives considered: 2MOA (Figure 2a), 3MOA (Figure 2b), MOMA (Figure 3a), and MMOA (Figure 3b).

Second, from the Mulliken population analysis we have estimated the net spin population of a given atom (say A) in a monomer as:

$$N_s(\mathrm{A}) = N_{\mathrm{A}\uparrow} - N_{\mathrm{A}\downarrow} \quad (2)$$

where $N_{A\uparrow}$ and $N_{A\downarrow}$ are the Mulliken net electron populations of the atom A for spin-up and spin-down directions, respectively. The sum of the latter two gives the corresponding total electron population of the atom A ($Q(\mathrm{A}) = N_{\mathrm{A}\uparrow} + N_{\mathrm{A}\downarrow}$). The difference between Q(A) in the neutral aniline and Q(A) in the radical cation estimates the accumulation of positive charge about a particular atom A in the radical cation. As seen from Table 2, the LSD and GGA atomic charges are very similar, with a maximum deviation of about 0.07, while the maximum deviation for the net spin populations N_s(A) is about 0.05 for the *para* carbon. The unpaired spin-density (assumed in the spin-up direction) is distributed among the atoms in a way resembling the inductive effect in such aromatic systems:[32] accumulation

Table 2. Calculated Atomic Net Spin Populations N_s(A) and Net Electron Populations Q(A) of the Aniline Radical Cation (Only the Symmetry Nonequivalent Carbon Atoms Are Presented)

method	atom	N_s(A)	Q(A)	δ^+(A)[a]
LSD	N	0.328	7.420	0.134
	C_1	0.127	5.585	0.057
	C_2(o)	0.154	6.182	0.070
	C_3(m)	−0.023	6.077	0.041
	C_4(p)	0.333	6.083	0.101
GGA	N	0.324	7.350	0.130
	C_1	0.128	5.632	0.060
	C_2(o)	0.169	6.141	0.069
	C_3(m)	−0.056	6.040	0.044
	C_4(p)	0.379	6.061	0.099

[a] δ^+(A) is the positive charge of a given atom in the radical cation obtained as a difference between Q(A) in the neutral aniline and Q(A) in the radical cation.

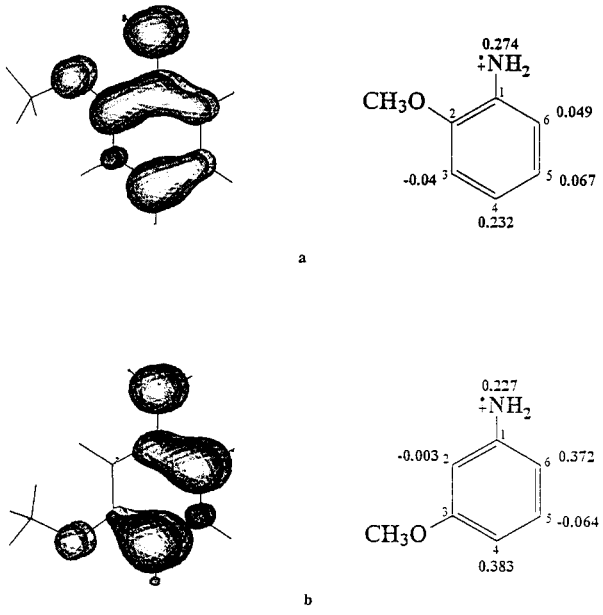

Figure 2. Unpaired-electron spin-density $n_s(\mathbf{r})$ for (a) 2MOA radical cation and (b) 3MOA radical cation. The darker surfaces (on one of the *meta* carbon atoms and on the hydrogen atoms of the *para* carbon of 3MOA) are at $n_s = -0.003$ au and the lighter surfaces are at $n_s = +0.003$ au. The corresponding values of the net atomic spin populations N_s(A) are denoted on the skeleton diagrams on the right.

(30) Hollas, J. M. *Modern Spectroscopy*; John Wiley and Sons: Chichester, 1987; p 110.

(31) Vosko, S. H.; Wilk, L.; Nusair, M. *Can. J. Phys.* **1980**, *58*, 1200.

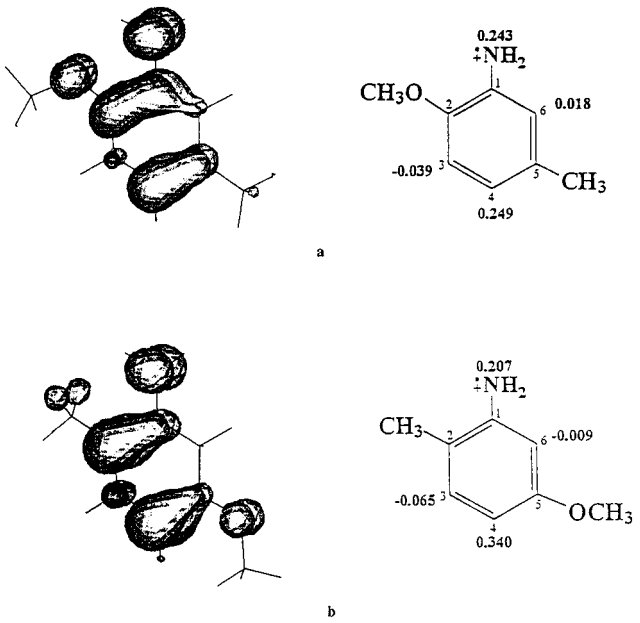

Figure 3. Unpaired-electron spin-density $n_s(\mathbf{r})$ for (a) MOMA radical cation and (b) MMOA radical cation. The designations of the isosurfaces and the skeleton diagrams are the same as in Figure 2.

of spin-up density around the ring carbon atoms at *ortho* and *para* positions, while depleting this density from the two *meta* carbon atoms (Table 2). The rules of electrophilic aromatic substitution may be applied to the distribution of the positive charge in the radical cation (the last column of Table 2): the NH_2 group is a well-known strong activating *ortho, para* director, promoting the induction of a positive charge at *ortho* and *para* positions.[32] This feature is reflected in our results for the atomic charges δ^+(A) (Table 2). We may assume that similar rules approximately hold for the net spin distribution in the benzenoid ring, since in the radical cations the positive charge distribution is closely related to the radical spin distribution. One should keep in mind though, that these two distributions might not always be in line: in the aniline radical cation the net atomic spin population N_s(A) of the ring carbon atoms follows closely the distribution of the positive radical charge δ^+(A), as can be seen from Table 2. However, comparing the values on the nitrogen atom and on the *para* carbon atom, one sees that $N_s(C_4(p))$ is slightly larger than N_s(N), whereas the positive charge on the nitrogen is greater than that on the $C_4(p)$ atom, at both the LSD and GGA levels. Note that the positive charge distribution is calculated using the electron population in the neutral aniline as a reference, and in a self-consistent manner, taking into account the geometry relaxation and symmetry breaking effects upon the radical cation formation. Overall, the calculated atomic net spins N_s(A) in the aniline radical cation form a kind of ordered structure, the spins on most of the carbon atoms being parallel (although different in magnitude) except for the two *meta*-carbon atoms. Since the trends in the electronic re-distribution upon forming the aniline radical cation are the same at both the LSD and GGA levels, we restrict our further analysis to the LSD level, which is less computationally demanding.

We have made a detailed comparison of the calculated electronic properties among the following two pairs of isomers: 2-methoxy-5-methylaniline versus 2-methyl-5-methoxyaniline on the one hand (Figures 3a, 3b), and 2-methoxyaniline versus 3-methoxyaniline on the other hand (Figures 2a and 2b).

(32) Morrison, R. T.; Boyd, R. N. *Organic Chemistry*; Allyn and Bacon, Inc.: Boston, 1983.

As was emphasized above, in both examples only one of the isomers gives electroactive polymers upon chemical or electrochemical oxidation (2-methoxy-5-methylaniline in the first example and 2-methoxyaniline in the second), while the oxidation of the corresponding counterpart does not lead to electroactive polymers.[14,16] Besides possible steric effects and the like, the question is whether there is a microscopic, electronically based cause for the difference in the polymerization activity of these isomers? This question has been addressed in previous studies of similar systems,[17,18] in terms of the electronegativity concept,[17] or the frontier orbital theory within the Hückel approximation.[18] We have analyzed and compared various calculated properties of the monomers: the orbital energies and the gap between the highest occupied molecular orbital (HOMO) and the lowest unoccupied one (LUMO), the total energies and the binding energies, the bond order of different bonds, the electron density and spin density distributions, and the corresponding atomic charge and spin populations of both the neutral monomers and the radical cations. Among these features we found one which seems to distinguish the polymerization-active from the polymerization-inactive monomers: the degree to which N_s(N) and $N_s(C_4(p))$ values are similar to each other, along with their absolute magnitude. In the active isomers, viz. when the alkoxy group is located at the 2-position (*ortho* carbon atom), the difference between the two net spins is relatively small: in 2-methoxy-5-methylaniline $N_s(N) = 0.243$, $N_s(C4(p)) = 0.249$ (Figure 3a); in 2-methoxyaniline $N_s(N) = 0.274$, $N_s(C_4(p)) = 0.232$ (Figure 2a). In the inactive forms, viz. when the alkoxy group is located either at the 3- or 5-positions (*meta* carbon atoms), the difference between N_s(N) and $N_s(C_4(p))$ is much larger, compared to that in the active isomers: in 2-methyl-5 methoxyaniline $N_s(N) = 0.207$, $N_s(C_4(p)) = 0.340$ (Figure 3b); in 3-methoxyaniline $N_s(N) = 0.227$, $N_s(C_4(p)) = 0.383$ (Figure 2b). The spin-density distribution is obviously related here to the position of the alkoxy group in the benzenoid ring and, consequently, to its electronic effects. The head-to-tail radical reaction can be considered as a special kind of electrophilic aromatic substitution at the $C_4(p)$ position. Both the alkoxy group and the methyl group belong to the category of activating *ortho, para* directors (as does the NH_2 group),[32] but the alkoxy group has a stronger directive power. In monomers like 3-methoxyaniline and 2-methyl-5-methoxyaniline (which are nonpolymerizable), the methoxy group is in the *meta* position with respect to the NH_2 group, and thus both groups reinforce each other to direct the unpaired spin density onto the $C_4(p)$ atom (which, with respect to the OCH_3 group, is in the *ortho* position). This explains why the net spin occupancy of the $C_4(p)$ atom is so enhanced in 3-methoxyaniline and 2-methyl-5-methoxyaniline (compared to the isomers having the OCH_3 group in the *ortho* position) and why the difference between N_s(N) and $N_s(C_4(p))$ is so large. The difference is relatively larger in 3-methoxyaniline than in 2-methyl-5-methoxyaniline (Figures 2 and 3), because the presence of a methyl group at the C_2 position (*ortho*) in the latter partly neutralizes the overall directive power of the other two groups, NH_2 and OCH_3. In both cases the monomers are nonpolymerizable, while in the polymerizable isomers the difference between N_s(N) and $N_s(C_4(p))$ is much smaller, which can be explained using similar substitution arguments. Thus, for the polymerizability a kind of an "equalization" condition emerges, concerning the atomic net spins on N and $C_4(p)$ atoms. In the considered processes, the polymerization is favored by a $C_4(p)-N$ binding between the monomers (head-to-tail), while the alternative C−C (tail-to-tail) and N−N (head-to-head) couplings give soluble and non-electroactive species.[33,34] A

suggestion as to why the $C_4(p)$−N binding occurs only in cases when $N_s(N) \approx N_s(C_4(p))$ may come by noticing that similar equalization conditions related to chemical reactivity are known within the (local) softness−hardness approach in DFT.[24] As stated in this approach, "hard" parts of a molecule tend to connect with "hard" counterparts in a reaction, while "soft" parts connect with soft counterparts. In DFT the local softness is defined by:[24]

$$s(\mathbf{r}) = \frac{\partial n(\mathbf{r})}{\partial \mu} \equiv \frac{\partial n(\mathbf{r})}{\partial N}\frac{\partial N}{\partial \mu} \tag{3}$$

where $n = n_\uparrow + n_\downarrow$ is the total electron density, N is the total number of electrons, and μ is the chemical potential of the molecule as defined in DFT by the following functional derivative:[24]

$$\mu = \frac{\delta E[n]}{\delta n} \tag{4}$$

In eqs 3 and 4 the derivatives are taken at fixed external potential v.

The two partial derivatives on the right-hand side of eq 3 have an important physical meaning: the derivative of the total number of electrons with respect to the chemical potential gives the global softness of the system[24]

$$S = \frac{\partial N}{\partial \mu} = \int s(\mathbf{r})\, \mathrm{d}\mathbf{r} \tag{5}$$

while the derivative of the electron density with respect to the total number of electrons defines the so-called Fukui function $f(\mathbf{r})$.[24] Equivalently, this function can be expressed through the variation (the response) of the chemical potential upon variation of the external potential (*i.e.* upon external perturbation).[24]

$$f(\mathbf{r}) = \left[\frac{\partial n(\mathbf{r})}{\partial N}\right]_v = \left[\frac{\delta \mu}{\delta v(\mathbf{r})}\right]_N \tag{6}$$

As is clear from eqs 3−6, the Fukui function is directly related to the local softness of the system:

$$s(\mathbf{r}) = f(\mathbf{r})\, S \tag{7}$$

The local softness, eqs 3 and 7, reflects local response properties of the valence electrons related to the magnitude of the local electron charge−charge fluctuations in different parts of the molecule.[24] These properties are substantially driven by electron correlation effects and have proven to be important factors in chemical reactivity. Similarly, the Fukui function itself has been used as a local reactivity index assuming that preferable sites for a reaction attack are those which produce the maximum chemical potential response to this attack.[24,35] One should note that in the simplest approximation to $f(\mathbf{r})$, the frozen core approximation, the Fukui function is given by the value of the orbital density of the HOMO (when the variation of N is taken from below) and by that of the LUMO (when the variation of N is taken from above). In this approximation the Fukui function approach recovers the frontier orbital theory of Fukui:[24,35,36] the orbital densities at HOMO and LUMO and their average value are measures for the reactivity toward electrophilic, nucleophilic, and radical-type reagents, respectively. In fact the more general Fukui function approach has been considered as a theoretical background of the frontier orbital theory, assuming that chemical reactions prefer the direction which produces maximum chemical potential response of a reactant.[35] Another approximation to $f(\mathbf{r})$ has been derived and considered particularly useful when radical-type reactions are concerned:[35] if one assumes that the variation of the electron density of a given spin upon an infinitesimal variation of the number of electrons with opposite spin is small (which is expected in most cases), then the Fukui function can be represented as proportional to the local spin-distribution function $n_s(\mathbf{r})$, eq 1, depicted in Figures 2 and 3:

$$f(\mathbf{r}) \cong \frac{n_s(\mathbf{r})}{N_s} \tag{8}$$

where N_s is the total spin of the system:

$$N_s = N_\uparrow - N_\downarrow = \sum_A N_s(A) \tag{9}$$

As is shown in ref 35, while energy changes during a reaction are governed by the total charge density, chemical potential changes are governed by the right-hand side of eq 8, *i.e.* by the unpaired spin-density. The known high reactivity of free radicals is associated with large spin-density gradients in these systems. According to eqs 6 and 8, this implies large gradients of their chemical potentials at the initial stage of the reaction (and hence large $f(\mathbf{r})$), and also large spin polarization and relaxation effects in the process of forming the radical. Since these effects are particularly important in radicals and radical cations, eq 8 is a more relevant approximation to the Fukui function for the systems considered than the simpler frozen core approximation, given by the HOMO (LUMO) densities. Nevertheless, as we shall see below in the case of the aniline cation, the two different approximations to the Fukui function lead to similar (although not identical) qualitative pictures. Integrating the unpaired spin density $n_s(\mathbf{r})$ over a properly defined atomic region gives the atomic net spin-population, which we estimate via the Mulliken population analysis. According to eq 8, the atomic net spin-population is proportional to the atomic Fukui function (the integral of $f(\mathbf{r})$ over the atomic region), which in turn is related to the atomic regional softness, via eq 7. Regarding the dimerization tendency of the considered monomers, the regional Fukui function represents directly the corresponding local softness, since the multiplier S in eq 7, *i.e.* the global softness, is the same for any two identical monomers at the initial stage of the dimerization (note that for the considered radical cations $N_s = 1$). So, the "soft goes to soft" principle[24] is in line with the equalization condition we observe: when the atomic softness of N is similar to that of $C_4(p)$, the desired head-to-tail binding ($C_4(p)$−N) of two monomers can successfully compete with the head-to-head and tail-to-tail bindings, thus opening the polymerization channel. According to eqs 7 and 8, an indication for such a situation is a similarity of the corresponding net atomic spin-populations: $N_s(C_4(p)) \approx N_s(N)$. In the opposite case (when $N_s(C_4(p))$ is noticeably different from $N_s(N)$), according to the same soft−soft principle, head-to-head (N−N) and tail-to-tail ($C_4(p)$−$C_4(p)$) couplings should prevail. Let us note that nonpolymerizable (N−N)- and (C−C)-type dimers may always be present as side products,[14] but only when $N_s(C_4(p)) \approx N_s(N)$ can the head-to-tail polymerization channel compete with them. Based on the softness equalization condition alone, one cannot estimate in detail whether and how much the head-to-tail channel is more favorable in this case. All we can state is that this channel

(33) (a) Doriomedoff, M.; Cristofini, F. H.; De Surville, R.; Jozefowicz, M.; Yu, L. T.; Périchon, J.; Buvet, R. *J. Chem. Phys.* **1971**, *68*, 1055. (b) Geniès, E. M.; Tsintavis, C. *J. Electroanal. Chem.* **1985**, *195*, 109.
(34) Hand, R. L.; Nelson, R. F. *J. Am. Chem. Soc.* **1974**, *96*, 850.
(35) Galvan, M.; Gazquez, J. L.; Vela, A. *J. Chem. Phys.* **1986**, *85*, 2337.
(36) Fukui, K. *Science* **1982**, *218*, 747.

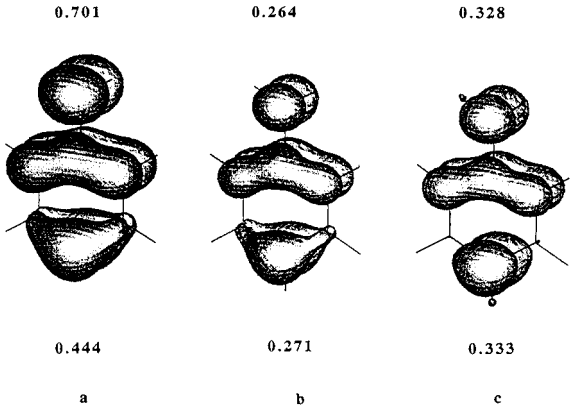

Figure 4. (a) the HOMO density in neutral aniline; (b) the HOMO density in the aniline radical cation at its optimized geometry; and (c) the unpaired-electron spin-density $n_s(\mathbf{r})$ of the aniline radical cation at its optimized geometry. The numbers denote the corresponding net atomic occupanices for the nitrogen atom (above) and for the *para* carbon atom (below).

should be at least equally probable. What the softness equalization condition definitely explains is why the polymerization is quenched when this condition is not obeyed.

Exploiting further these concepts, we notice that for the aniline radical cation (which is also very polymerizable) (Table 2 and Figure 4) $N_s(N) = 0.328$ and $N_s(C_4(p)) = 0.333$, *i.e.* again the softness equalization condition is fulfilled. However, we observe here that the magnitude of $N_s(C(ortho))$ is also appreciable (0.154), that means appreciable atomic Fukui function on the *ortho* C atom, which opens a possibility for additional side-couplings at the *ortho* position.[33,34]

In the particular case of aniline, we have studied also the similarities and the differences between the two different approximations to the Fukui function: the frozen core approximation (the HOMO orbital density) vs eq 8 (the unpaired spin-density). Figure 4 depicts the spin-density n_s in the aniline radical cation (Figure 4c), as well as the (majority-spin) HOMO orbital density in this cation (Figure 4b), and in neutral aniline (Figure 4a). Comparing first the distribution of the HOMO density in the aniline radical cation with that in neutral aniline, Figure 4a,b, it is seen that the shapes are qualitatively similar. However, an important quantitative difference is also observed: in neutral aniline (Figure 4a) the net HOMO orbital occupancy on the nitrogen atom (via the Mulliken orbital population analysis) is 0.701, and much larger than that of the *para* carbon atom, which is 0.444. Simplified quantum chemical treatments of the radical cation, in which the HOMO orbital is kept frozen during the radical formation (*i.e.* neglecting the orbital and geometry relaxation, and effects of the spin polarization in the cation), would give a ratio similar to Figure 4a between the net HOMO occupancy on N and C(*p*) atoms. Such is, for example, the case of using the semiempirical extended Hückel method[18] to estimate the HOMO density distribution in the aniline radical cation. Taking into account the orbital and the geometry relaxation and the spin polarization effects in a self-consistent manner leads to a noticeable change in the ratio between the HOMO occupancy on N and C(*p*) atoms, Figure 4b: 0.264 on the nitrogen atom and 0.271 on the *para* carbon atom, that is, a redirection of HOMO density from the nitrogen atom to the *para* carbon atom when going from neutral aniline to the radical cation. On the other hand, comparing the HOMO density distribution and the unpaired-electron spin-density distribution in the aniline radical cation (both obtained in a self-consistent manner), Figure 4b,c, it is seen that the two approximations to the Fukui function give qualitatively very similar pictures for the contributions from the N and C(*p*) atoms, as long as full self-consistency is attained in both calculations. However, differences between the two approximations still exist: by using the spin-density distribution n_s, one takes also into account the relaxation and spin polarization of the inner occupied orbitals. In the present work we use eq 8 as a more representative approximation to the Fukui function in our analysis of the softness equalization condition and its relation to the polymerizability of the considered aniline derivatives.

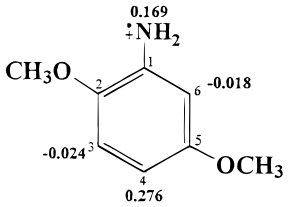

Figure 5. Net atomic spin populations $N_s(A)$ for the oxidized 2,5-dimethoxyaniline (DMOA).

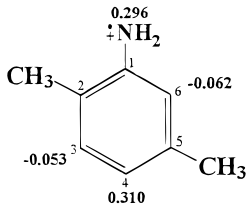

Figure 6. Net atomic spin populations $N_s(A)$ for the oxidized 2,5-dimethylaniline (DMA).

Of course, the softness equalization condition proposed here does not reflect all the details of the polymerization process. In reality, the polymerization reactions are very complicated, multistep processes. However, the aspect considered here, namely the step where the radical cation couples to the polymer, is clearly a crucial one. Other aspects have, indeed, been considered in formulating the present study. Certainly, to attain a more complete picture one should consider for example the effect of the solvent acidity on the regioselectivity of the coupling between the monomers.[18] However, as described in ref 14, we have tried various different solvents and conditions for the considered polymerization processes, but the nonpolymerizable monomers always remained nonpolymerizable. We believe that the main reasons for this phenomenon are connected with the specific electronic structure of the radical cations, which was the motivation of the present theoretical study. The primary importance of the electronic structure of radical cations in polymerization processes has been emphasized also in refs 18 and 19.

Considering the other compounds studied, in dimethoxyaniline (Figure 5), $N_s(N) = 0.169$, while $N_s(C_4(p)) = 0.276$. In practice this monomer is active, although the observed polymerization is not so regular and noticeable formation of inactive dimers (with N−N and C−C couplings) has been detected.[37] This could be explained by the obtained deviation from the softness equalization condition for this monomer.

In the last example, 2,5-dimethylaniline, $N_s(N) = 0.296$ and $N_s(C_4(p)) = 0.310$ (Figure 6), and the softness equalization condition is well obeyed. In practice, however, the synthesis of this polymer meets difficulties,[38] which might be associated with steric effects.

One should also keep in mind that the Mulliken approximation for the atomic net spin population has its own limitations, and spurious side effects associated with this approximation,

(37) Zotti, G.; Comisso, N.; D'Aprano, G.; Leclerc, M. *Adv. Mater.* **1992**, *4*, 749.

(38) Geniès, E. M.; Noel, P. *J. Electroanal. Chem.* **1990**, *296*, 473.

Table 3. LSD Bond Distance and Bond Order between the Oxygen Atom from the OCH_3 Group and the Hydrogen Atom from the NH_2 Group in the Monomers Having a Methoxy Group at the *Ortho* Position

compd[a]	$P_{O\cdots H}$	$R_{O\cdots H}$ [Å]
2MOA^o	0.0301	2.1803
2MOA$^+$	0.0249	2.2015
MOMA^o	0.0296	2.1900
MOMA$^+$	0.0249	2.1990
DMOA^o	0.0270	2.2380
DMOA$^+$	0.0236	2.1976

[a] The abbreviations of the monomers are the same as in the text.

as well as basis set limitations and the approximations of the method used, may influence the results. Therefore caution is needed when comparing the calculated values of N_s, keeping in mind that the numbers may change slightly with a change of the basis set or the method used. The real space distribution of the local spin function (Figures 2 and 3) provides a useful complementary picture in this respect, since this distribution has proven to be relatively more stable with respect to such changes. Comparing the distribution of the excess spin around the N and $C_4(p)$ atoms, one can envisage from these pictures the softness equalization condition in terms of difference in the size of the "spin clouds" around N and $C_4(p)$ atoms. Indeed, in the case of 3MOA (Figure 2b) and MMOA (Figure 3b), the spin cloud on the $C_4(p)$ atom looks slightly larger than the one on the nitrogen. Other differences between the active and inactive species can also be seen in Figures 2 and 3. For example, the spin cloud on the $C_4(p)$ atom of the active monomers (2MOA, Figure 2a, and MOMA, Figure 3a) is more evenly distributed over these atoms and one of the neighboring *meta* carbon atoms. Similarly, the spin cloud on the carbon atom carrying the aniline substituent is spread over both *ortho* carbon atoms in the active monomers, while it is spread only on one of them in the inactive species. Note also that only the inactive monomers have negative N_s value on the hydrogen atoms of the *para* carbon atom. Of course, the exact shape of the spin clouds depends on the precise value chosen for N_s, but it remains that similarities and differences between these shapes can be observed for the inactive and the active species.

It is perhaps worth pointing out that for the monomers with a methoxy group at the *ortho* position, one might wonder whether an internal hydrogen bond could form between the oxygen atom from the methoxy group and a hydrogen atom from the NH_2 group. This might potentially create a concern for the validity of the present calculations because the LSD approximation is known to overestimate the strength of hydrogen bonds and underestimate the corresponding bond lengths.[39] If such effects were strong, then the overall electronic structure might be unduly perturbed. For example, the LSD O···H bond in the water dimer is too short by 0.25 Å and the O···H bond order is too large by a factor of 2. Similar trends were found for the HF dimer as well.[39] To address this question we have calculated the O···H bond orders in the monomers in question, and these are presented along with the O···H distances in Table 3. The numbers could correspond to long, weak hydrogen bonds. However, given the LSD trends mentioned above, these should be regarded as, if anything, overemphasizing hydrogen bonding. Therefore, it is safe to conclude that internal hydrogen bonding in the considered species would be even weaker than what is indicated by the figures in Table 3, and hence need not be of concern.

Conclusions

The present DFT study of a series of aniline derivatives provides insight into their potential polymerizability. The DFT approach not only yields numerical results for the electronic and geometric structure of the monomers, but also allows for a conceptual interpretation of the observed correlation between the polymerization activity and the atomic net spin populations in the radical cations. The equalization condition which emerges from our calculations, namely the condition that $N_s(N) \approx N_s(C_4(p))$ for a monomer to be active in polymerization, can be explained as a particular realization of the soft−soft reactivity principle in DFT.

We emphasize that the present model concerns only the first step of the polymerization process, the coupling between monomers. This of course does not provide a complete description of the whole radical reaction, which in reality is certainly a complicated multiaspect phenomenon. More sophisticated models and calculations involving larger fragments of the polymer chain would be necessary to describe the reaction more fully. However, the $N_s(N) \approx N_s(C_4(p))$ condition emerges as a necessary one and this principle should help to guide future syntheses. If the condition is not satisfied polymerization will not occur. If it is, then a rapid addition of the highly reactive radical cation to the growing polymer chain is to be expected.

As was also concluded in ref 19, contemporary quantum-chemical methods can be successfully used as a predictive tool in the design of novel conducting polymers.

Acknowledgment. The authors gratefully acknowledge financial support from NSERC and computing resources from the Services Informatiques de l'Université Montréal and CERCA (Centre de Recherche en Calcul Appliqué). The authors thank A. Vela for illuminating discussions about the Fukui function and the local softness concept. G.D.A. is grateful to NSERC and FCAR programs for graduate fellowships.

JA953819Z

(39) Salahub, D. R.; Proynov, E. E.; Vela, A.; Ruiz, E. In *New Methods in Quantum Theory*; NATO ASI Series; Tsipis, C. A., Popov, V. S., Herschbach, D. R., Avery, J., Eds.; Kluwer: Dordrecht, 1996; p 359. Salahub, D. R., Proynov, E., Unpublished.